Electrical Resistivity Versus Deuterium Concentration in Palladium

G. BAMBAKIDIS, R. J. SMITH, AND D. A. OTTERSON
Lewis Research Center, National Aeronautics and Space Administration, Cleveland, Ohio 44135
(Received 25 July 1968)

The electrical resistivity of the palladium-deuterium system has been measured up to a deuterium-to-palladium atom ratio of 0.9 at temperatures of 273, 77, and 4.2 K. The resistivity ratio ρ_x/ρ_0 was plotted versus the atom ratio x at 273 and 4.2 K. The structural resistivity has been calculated, assuming two types of scattering centers associated with the deuterium having widely different screening radii. A good fit with the data at 4.2 K is obtained by assuming that the number of d holes per Pd atom takes on the value 0.55–0.60 upon addition of deuterium.

INTRODUCTION

IT has been shown that at room temperature deuterium (or hydrogen) occupies the octahedral interstitial sites of the fcc Pd lattice.[1,2] The octahedral sites are occupied for both α-Pd and β-Pd with the D/Pd and H/Pd atom ratios ranging from zero to 0.72 (here α-Pd and β-Pd have lattice constants of 3.89 and 4.02 Å, respectively). Denoting the D/Pd or H/Pd atom ratios by x, it is found that only α-Pd exists for $0<x\lesssim 0.02$. For $0.02\lesssim x\lesssim 0.60$ α-Pd and β-Pd coexist, and only β-Pd is found for $x\gtrsim 0.60$. If ρ_x is the resistivity of PdH_x (or PdD_x) and ρ_0 is the resistivity of annealed Pd, then the resistivity ratio $(\rho_x/\rho_0)_{298\text{ K}}$ and its derivative increase for increasing x for $0.02\lesssim x\lesssim 0.70$. The resistivity ratio is a maximum for $x\simeq 0.76$ and the ratio along with its derivative decreases for $0.76\lesssim x\lesssim 0.88$.[3] In the PdD_x system, the available data show $(\rho_x/\rho_0)_{298\text{ K}}$ and its derivative increase from $x\simeq 0.02$ to $x=0.67$ with no higher values of x being shown.[4] For pure α-Pd ($x\lesssim 0.02$), the derivative of the resistivity ratio $(\rho_x/\rho_0)_{298\text{ K}}$ is larger than that for the α-Pd+β-Pd phase for either PdH_x or PdD_x.

The object of this work is to attempt to understand the structural part of the resistivity of PdD_x and PdH_x. We have chosen PdD_x instead of PdH_x because it appears to be easier to maintain the room-temperature structure of β- and (α+β)-Pd at 4.2 K for PdD_x than for PdH_x. It will also permit us to see if a maximum occurs in the plot of ρ_x/ρ_0 versus x for PdD_x for $x>0.67$. We minimize the thermal contribution to the resistivity by obtaining data at 4.2 K and then use a modification of Mott's model for the resistivity of transition metal alloys[5] for the analysis of the structural contribution. The resistivity results and analysis presented here for the PdD_x system should be qualitatively applicable to the PdH_x system since these systems are quite similar in other resistive and crystallographic properties thus far investigated.[1–4,6–8]

EXPERIMENTAL

The experimental data were obtained at 4.2, 77, and 273 K. In obtaining the 4.2 K data it was necessary to rapidly cool or quench the PdD_x wires from 273 to 4.2 K in order to prevent the migration of D ions from their octahedral sites (0, 0, $\frac{1}{2}$; 0, $\frac{1}{2}$, 0; $\frac{1}{2}$, 0, 0; etc.) to tetrahedral sites ($\frac{1}{4}$, $\frac{1}{4}$, $\frac{1}{4}$; $\frac{3}{4}$, $\frac{3}{4}$, $\frac{3}{4}$; etc.). An analysis of neutron-diffraction and resistivity-versus-temperature (ρ-versus-T) data for PdH_x show that up to 25% of the H may migrate to tetrahedral sites. These octahedral-tetrahedral transitions occur for PdH_x for $0.45<x<0.75$ if the PdH_x wires are cooled without quenching.[6,7] In the PdH_x system the octahedral-tetrahedral transitions may begin well above 100 K and continue at least to the neighborhood of 50 K (at which point a maximum in the resistivity and specific heat occurs) as the temperature is lowered from 273 to 4.2 K.[6] (It is not known whether or not additional transitions occur below these maxima.) While no neutron-diffraction data are available for PdD_x the resistivity data of PdD_x are almost identical to those obtained for PdH_x between 273 and 4.2 K.[8] However, at a given temperature, the octahedral-tetrahedral transitions take much longer in the PdD_x system (up to several hours) than in the PdH_x system (not more than a few seconds). From these data for PdD_x, one can conclude that rapid cooling of the PdD_x specimens from 298 to 4.2 K, as employed in our present experiments, was sufficient to prevent a significant amount of deuterium migration to the tetrahedral sites.

Wire specimens of 99.995 at.% Pd (manufacturer's stated purity) and 0.254-mm diam were annealed by Joule heating in a vacuum of 5×10^{-9} Torr at approximately 950 C for at least 0.5 h. Initial resistivity, ρ_0, measurements were made at 4.2, 77, and 273 K by using the conventional four-probe potentiometric technique with a Bakelite specimen holder utilizing phosphor-bronze spring contacts for the current and potential contacts to the specimen. There were a total of six potential contacts spaced 1 cm apart between the

[1] J. E. Worsham, M. G. Wilkinson, and C. G. Schull, J. Phys. Chem. Solids **3**, 303 (1957).
[2] A. J. Maeland, Can. J. Phys. **46**, 121 (1968).
[3] J. C. Barton, F. A. Lewis, and I. Woodward, Trans. Faraday Soc. **59**, 1201 (1963).
[4] T. B. Flanagan, J. Phys. Chem. **65**, 280 (1961).
[5] N. F. Mott and H. Jones, *The Theory of the Properties of Metals and Alloys* (Dover Publications, Inc., New York, 1958), pp. 296ff.
[6] A. I. Schindler, R. J. Smith, and E. W. Kammer, in *Proceedings of the Tenth International Congress of Refrigeration* (Pergamon Press Ltd., London, 1960), Vol. 1, p. 74.
[7] G. A. Ferguson, A. I. Schindler, T. Tanaka, and T. Morita, Phys. Rev. **137**, A483 (1965).
[8] R. J. Smith, NASA Report No. TN D-2568, 1965 (unpublished).

current contacts, permitting five consecutive measurements along the wire which allowed detection of resistance irregularities due either to preabsorption conditions and/or nonuniform absorption along the wire after D absorption. The measuring currents used were 10 mA in all cases.

Deuterium absorption was accomplished electrolytically, using a graphite anode and the Pd wire as the cathode in a 1N D_2SO_4 solution and 5-mA current. The anode and cathode were separated by a porous alumina crucible, as shown in Fig. 1, in order to prevent oxidizing agents that may be formed at the anode from reaching the cathode, thereby permitting the Pd to absorb higher concentrations of deuterium. Immediately after the absorption process, the wires were returned to the Bakelite holder for resistivity measurements at 4.2, 77, and 273 K to obtain ρ_x (or R_x).

In order to determine the D/Pd atom ratios, each specimen was sectioned into five 1-cm pieces which corresponded to the positions on the Bakelite specimen holder. Then the deuterium was removed from each centimeter section by separately heating each section to 300 C in an evacuated system ($\sim 10^{-6}$ Torr). Tests showed that of the gases, less than 1% generally remained in the specimens. The specimens were weighed to three significant figures. The deuterium was expanded into and analyzed with a mass spectrometer which is capable of 1% precision. The D/Pd atom ratios were then compared to their respective resistivity measurements.

RESULTS

The 4.2 and 273 K results are shown in Figs. 2(a) and 2(b). In Fig. 2(a) it can be seen that ρ_x/ρ_0 and its derivative increase with x for $0.02<x<0.65$ with $(\rho_x/\rho_0)_{273\text{ K}}$ reaching a maximum in the neighborhood of $x\simeq 0.72$ then decreasing as $x\rightarrow 0.90$. At 4.2 K, the maximum in $(\rho_x/\rho_0)_{4.2\text{ K}}$ appears to be near 0.68 D/Pd atom ratio.

Some of the scatter in the data may be attributed to two sources: (a) some hydrogen contamination which varied between 3 and 8% of total gas concentration and (b) some evolution of the absorbed D, for $x>0.7$, between the resistivity measurements and mass-spectrographic analysis. The time period for which evolution could take place was less than 20 min. (There is no evidence that evolution occurs at or below 77 K.) The possible gas loss for this time period is approximately 0.025 D/Pd atom ratio, which is equivalent to a 2% change in ρ_x/ρ_0 at 273 K. The data shown in Figs. 2(a) and 2(b) include both D and the H impurity in x [i.e., (D+H)/Pd].

DISCUSSION

In Fig. 2(a) an experimental curve has been drawn through the data points, while the curves in Fig. 2(b)

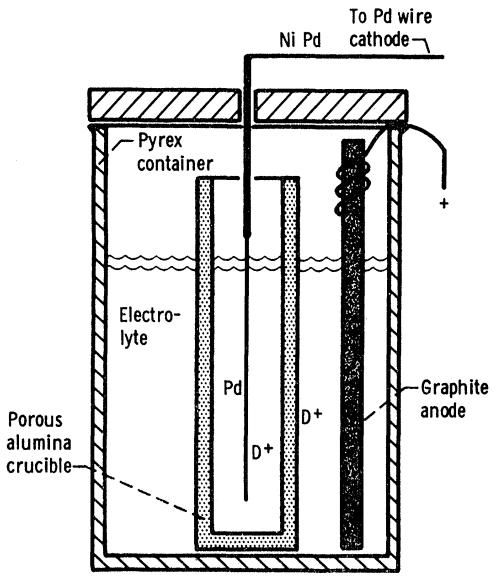

FIG. 1. Container used for deuterium absorption by Pd.

were calculated for the number of holes (n_h) per Pd atom in the d band being 0.36 and 0.55. (We do not give the results for 77 K since some octahedral-tetrahedral transitions occur during measurement.) The difference in the data at the two temperatures shown is attributed to the thermal contribution to the resistivity. At 4.2 K we expect both the thermal resistivity and that arising from lattice defects to be small, so that their variation with D concentration can be neglected. If x denotes the D/Pd atom ratio, the resistivity ratio $\rho(x)/\rho(0)$ at this temperature can therefore be written

$$\rho(x)/\rho(0)=1+\rho_D(x)/\rho(0), \qquad (1)$$

where $\rho_D(x)$ is the contribution from disorder scattering by the deuterium randomly distributed among the octahedral sites in the host fcc Pd lattice. This is also the resistance ratio since the change in sample dimensions due to lattice expansion upon absorption of D is negligible here. The average value of $\rho(0)$ for the samples used was determined to be 0.105 $\mu\Omega$ cm.

Magnetic susceptibility[9] and electromigration[10] studies on the Pd-H system indicate that H exists in the Pd lattice as strongly screened positive ions, and presumably the same situation exists for D. To describe the electronic structure of pure Pd we use the Mott model,[9] in which it is assumed that the band structure consists of a broad free-electron-like s band overlapping with a narrow d band such that the Fermi level occurs near the top of the d band. Thus there are electrons in the s band and an equal number of holes in the d band. We assume that initially the D atoms

[9] See Ref. 5, pp. 189ff.

[10] R. M. Barrer, *Diffusion in and Through Solids* (Cambridge University Press, Cambridge, England, 1941), p. 220.

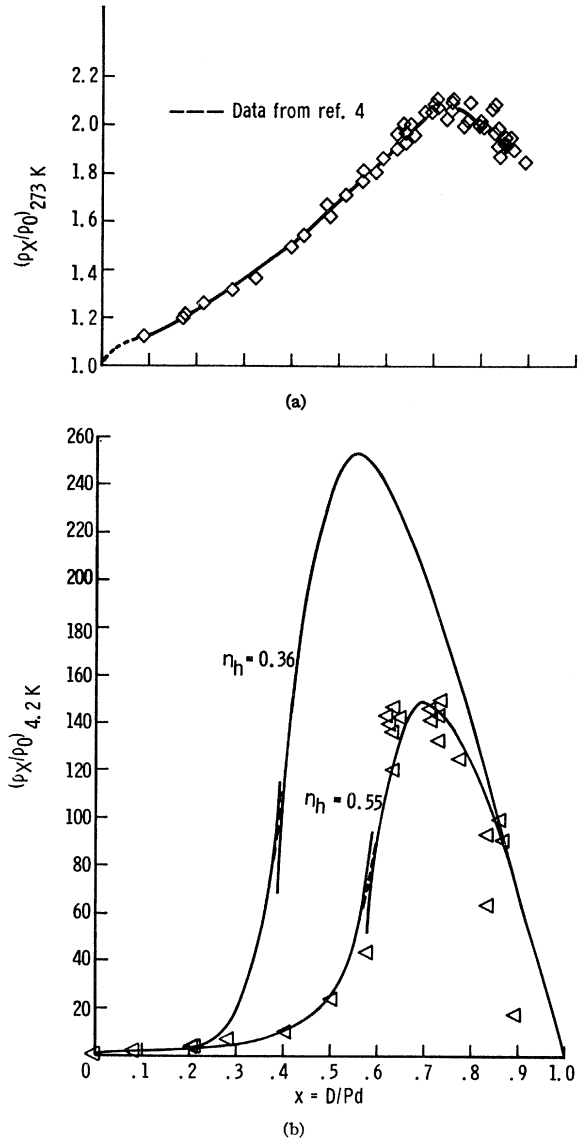

FIG. 2. (a) Resistivity ratio at 273 K versus D/Pd atom ratio—experimental curve. (b) Resistivity ratio at 4.2 K—calculated curves for number of d-band holes equal to 0.36 and 0.55.

contribute their electrons to filling the holes in the d band. In a covalent bond picture we can think of the electron as being shared with neighboring Pd atoms, resulting in a strong screening of the D ion. The D ions therefore scatter a conduction electron only weakly, giving rise to a small initial slope (the change in slope upon appearance of the β phase, observed at higher temperatures, is greatly diminished at 4.2 K, suggesting that its origin is thermal rather than structural). As the holes in the d band are filled the electrons are contributed instead to the s band, whose states are delocalized and hence do not screen as strongly. This results in the sharp rise in resistance. We thus view the resistance as arising from scattering by three types of local structure, denoted by I, II, and III in the potential-energy diagram of Fig. 3. Each of the three types is distributed randomly throughout the system. The screened Coulomb potentials about the D ions have screening lengths a_d and a_s, with $a_d<a_s$.

If we neglect the current carried by the holes, then the Boltzmann-equation approach and the assumption of an isotopic relaxation time τ lead to the usual expression

$$\rho=m_e^*/N_e e^2\tau, \tag{2}$$

where m_e^* is the effective mass and N_e is the number of conduction electrons per unit volume. We can write

$$\frac{1}{\tau}=\frac{1}{\tau_{s-s}}+\frac{1}{\tau_{s-d}}, \tag{3}$$

but the contribution from s-d scattering, being proportional to the density of states at the Fermi level, goes to zero as the d band fills. We therefore believe that s-d scattering cannot play a significant role in the sharp rise in $\rho(x)/\rho(0)$ with x, and we neglect it.[11]

When $1/\tau_{s-s}$ is evaluated in the Born approximation, the result for $\rho_D(x)$ is (see Appendix)

$$\rho_D(x)=\frac{2}{3\pi}\frac{(m_e^*)^2e^2}{\hbar^3}\frac{\Omega_0(x)}{[n_e(x)]^2}[f(4k_F^2a_d^2)x_d(1-x_d) +f(4k_F^2a_s^2)x_s(1-x_s)+2g(k_F,a_d,a_s)x_dx_s]. \tag{4}$$

The quantity $n_e(x)$ is the number of electrons per Pd atom in the s band, and $\Omega_0(x)$ is the volume per Pd atom, which is weakly dependent upon x because of lattice expansion. Because the exact variation of lattice parameter with concentration is not important here, a simple linear expansion of the lattice parameter from 3.88 Å at $x=0$ to 4.02 Å at $x=0.60$ is assumed. The quantities x_d and x_s denote the number of D atoms per Pd atom contributing an electron to the d band and s band, respectively. Both depend implicitly on the total concentration x. The Fermi wave vector k_F is given by

$$k_F=[3\pi^2n_e(x)/\Omega_0(x)]^{1/3},$$

while f and g are defined by

$$f(4k_F^2a^2)=\ln(1+4k_F^2a^2)-4k_F^2a^2/(1+4k_F^2a^2)$$

and

$$g(k_F,a_d,a_s)=\frac{a_s^2\ln(1+4k_F^2a_d^2)-a_d^2\ln(1+4k_F^2a_s^2)}{a_s^2-a_d^2}.$$

Equation (4) cannot be expected to be valid in the upper range of concentration (at and above the maxi-

[11] While s-d scattering does contribute at low concentrations, we expect that even here its effect is diminished compared with that in substitutional alloys such as Pd-Ag, since the scattering potential is centered on a D ion while its matrix element, which enters into $1/\tau_{s-d}$, is taken between an s state and a d state which is centered on a Pd ion.

mum in $[\rho(x)/\rho(0)]_{4.2\text{ K}}$) because we have not taken into account the development of long-range order near $x=1$, where the system takes on the NaCl structure. It therefore overestimates the resistance in this range. If at $x=1$ we regard the strongly screened and weakly screened D ions as constituting independent superlattices then the resistance for $x\lesssim 1$ will arise from scattering by type-II and -III structures only. Proceeding as before results in the high charge expression (see Appendix)

$$\rho_D(x)=\frac{2}{3\pi}\frac{(m_e^*)^2e^2}{\hbar^3}\frac{\Omega_0(x)}{[n_e(x)]^2}f(4k_F^2a_s^2)\frac{(x-n_h)(1-x)}{1-n_h}, \quad (5)$$

where $x\gtrsim n_h$. The parameter n_h is the number of holes per Pd atom in the d band at the initiation of charging, hence also the number of octahedral sites per Pd atom available to the strongly screened D ions. The assumption of independent superlattices means that Eq. (5) underestimates the resistance in the range $x\gtrsim n_h$.

We expect x_d, x_s, and n_e to have the qualitative behavior shown in Fig. 4. We note that $x_d+x_s=x$ and $n_e(x)=n_e(0)+x_s$. The concentration x_f is that at which the d band fills, and experiments by others[5] on palladium-noble metal alloys indicate this to be in the region of 0.55–0.60. On the basis of the de Haas–van Alphen (dHvA) measurements of Vuillemin[12] on pure Pd, $n_e(0)=0.36$. If this value is also used for the number of holes, we get the curve indicated in Fig. 2(b). The dashed line indicates the continuous curve which would come out of a more exact treatment of the onset of long-range order. The effective mass used, assumed independent of composition, was an average band mass of 0.49 m_e obtained from k_F and E_F for pure Pd. E_F was taken as 0.462 Ry, using Segall's[13]

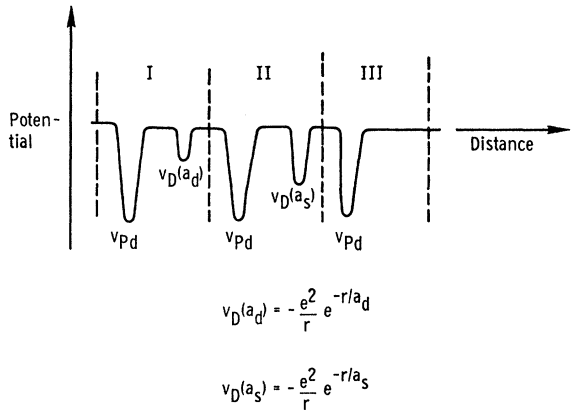

FIG. 3. The three types of local structure assumed present in the Pd-D system. (I) a Pd atom associated with a strongly screened D ion, screening length a_d; (II) a Pd atom associated with a weakly screened D ion, screening length a_s; (III) a Pd atom associated with a vacancy.

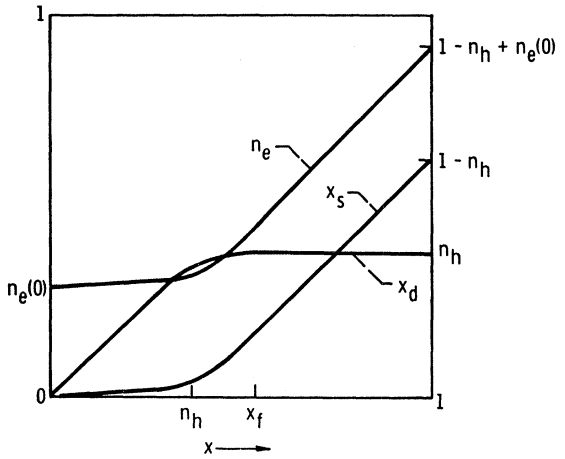

FIG. 4. Expected x dependence of the quantities x_d, x_s, and n_e entering into Eqs. (4) and (5).

band-structure calculations for copper and the similarity in the band structures of Pd and Cu.[12] The quantity x_f was taken as 0.60, and a_d and a_s were determined by fitting Eqs. (4) and (5) to the initial and (extrapolated) final slopes, respectively. The fit over the entire concentration range is certainly not quantitative, but if we assume that the number of holes in the d band increases from 0.36 upon charging, a much better fit is obtained as shown by the second curve ($n_h=0.55$). Values for n_h in the range 0.55–0.60 are consistent with magnetic-susceptibility data obtained by others on Pd-H.[5] The values for the screening lengths are $a_d=0.26$ a.u., and $a_s=1.11$ a.u. (at $x=1$). This value for a_s is somewhat larger than the Thomas-Fermi value of 0.74 a.u.

We are aware that the assumption of a spherical s-electron Fermi surface neglects the appreciable anisotropy, which ranges up to about 30%.[12] However, the Mott model, with the interpretation of the dHvA work that $n_e(0)=n_h(0)=0.36$, appears to work well in explaining the transport properties of the Pd-noble metal alloys.[14] The apparent failure of the rigid-band model for Pd-D indicated here suggests that further work on this system would be of interest. In particular, a band-structure calculation could be done for the ordered structure $x=1$ to obtain $n_e(1)$. The rigid-band model predicts one s electron per Pd atom at D/Pd or H/Pd=1, while the present analysis would indicate 0.81 electron per atom. In conjunction a dHvA experiment could be carried out. This would depend, however, on overcoming present experimental difficulty in consistently obtaining high D/Pd ratios.

APPENDIX

The expression for the inverse of the relaxation time $\tau_{s\text{-}s}$ for scattering of an s electron at the Fermi surface

[12] J. J. Vuillemin, Phys. Rev. **144**, 396 (1966).
[13] B. Segal, Phys. Rev. **125**, 109 (1962).
[14] J. S. Dugdale and A. M. Guénault, Phil. Mag. **13**, 503 (1966).

back into an s state by a single scatterer is[15]

$$\frac{1}{\tau_{s-s}}=\frac{\Omega}{4\pi^2\hbar}\int_{s\text{ surface}} dS(1-\cos\theta)\,|v_{\mathbf{k}'\mathbf{k}}|^2\frac{1}{|\nabla E_F|}$$
$$=\frac{\Omega}{2\pi\hbar}k_F^2\left(\frac{dE}{dk}\right)^{-1}_{k=k_F}\times\int_0^\pi d\theta(1-\cos\theta)\sin\theta\,|v_{\mathbf{k}'\mathbf{k}}|^2. \quad \text{(A1)}$$

The integral is taken over all scattering angles θ between the initial state $\mathbf{k}$ and final state $\mathbf{k}'$. The matrix element $v_{\mathbf{k}'\mathbf{k}}$ is

$$\int_\Omega d\mathbf{r}\phi_{\mathbf{k}'}{}^*(\mathbf{r})v(\mathbf{r})\Psi_{\mathbf{k}}(\mathbf{r}),$$

where $\Psi_{\mathbf{k}}$ is the initial state in the presence of the scattering potential $v(\mathbf{r})$ and $\phi_{\mathbf{k}'}$ is the final state in the absence of v. We assume the s-band wave functions can be taken as plane waves. In the Born approximation, $\Psi_{\mathbf{k}}$ is taken equal to $\phi_{\mathbf{k}}$ in evaluating $v_{\mathbf{k}'\mathbf{k}}$. Hence

$$v_{\mathbf{k}'\mathbf{k}}=\frac{1}{\Omega}\int_\Omega d\mathbf{r}e^{-i(\mathbf{k}'-\mathbf{k})\cdot\mathbf{r}}v(\mathbf{r}). \quad \text{(A2)}$$

Since a perfectly periodic potential has no resistance, we consider the contribution from each type of local structure of Fig. 3 as arising from the difference between the actual potential and the average potential there. The latter is

$$v_{\text{av}}=[v_{\text{Pd}}+v_{\text{D}}(a_d)]x_d+[v_{\text{Pd}}+v_{\text{D}}(a_s)]x_s+v_{\text{Pd}}(1-x_d-x_s).$$

Hence the scattering potentials are

$$\text{(I)}\quad v(\mathbf{r})=v-v_{\text{av}}=[v_{\text{Pd}}+v_{\text{D}}(a_d)]-[v_{\text{Pd}}+x_dv_{\text{D}}(a_d)+x_sv_{\text{D}}(a_s)]=(1-x_d)v_{\text{D}}(a_d)-x_sv_{\text{D}}(a_s),$$

and similarly

$$\text{(II)}\quad v(\mathbf{r})=(1-x_s)v_{\text{D}}(a_s)-x_dv_{\text{D}}(a_d);$$
$$\text{(III)}\quad v(\mathbf{r})=-x_dv_{\text{D}}(a_d)-x_sv_{\text{D}}(a_s).$$

The total contribution to $1/\tau_{s-s}$ from each type of scatterer consists of a term of the form (A1) with the appropriate scattering potential, weighted by the number of each type. Denoting matrix elements by $(\langle\ \rangle)$ and integration over the scattering angle by $(\ )_{\text{av}}$, we obtain

$$\frac{1}{\tau_{s-s}}=\frac{\Omega N_{\text{Pd}}}{2\pi\hbar}k_F^2\left(\frac{dE}{dk}\right)^{-1}_{k=k_F}\times\{(|\langle v_{\text{D}}(a_d)\rangle|^2)_{\text{av}}x_d(1-x_d)+(|\langle v_{\text{D}}(a_s)\rangle|^2)_{\text{av}}x_s(1-x_s)+2(\text{Re}[\langle v_{\text{D}}(a_d)\rangle\langle v_{\text{D}}(a_s)\rangle^*])_{\text{av}}x_dx_s\}, \quad \text{(A3)}$$

where N_{Pd} is the number of Pd atoms in the system. The appropriate integrals can be evaluated straightforwardly, resulting in Eq. (4).

In the high-charge region we assume the resistance arises mostly from the presence of vacancies in a superlattice of weakly screened D ions. The scattering arises from fluctuations in an average potential

$$v_{\text{av}}=\frac{1}{1-n_h}v_{\text{Pd}}+\frac{x_s}{1-n_h}v_{\text{D}}(a_s)+\frac{x_d}{1-n_h}v_{\text{D}}(a_d).$$

The scattering potentials are now

$$\text{(II)}\quad v(\mathbf{r})=\left(1-\frac{x_s}{1-n_h}\right)v_{\text{D}}(a_s);$$

$$\text{(III)}\quad v(\mathbf{r})=-\frac{x_s}{1-n_h}v_{\text{D}}(a_s).$$

There are x_s type-II scatterers and $1-n_h-x_s$ type-III scatterers per Pd atom. Therefore,

$$\frac{1}{\tau_{s-s}}=\frac{\Omega N_{\text{Pd}}}{2\pi\hbar}k_F^2\left(\frac{dE}{dk}\right)^{-1}_{k=k_F}\times\left[(|\langle v_{\text{D}}(a_s)\rangle|^2)_{\text{av}}\left(1-\frac{x_s}{1-n_h}\right)^2x_s+(|\langle v_{\text{D}}(a_s)\rangle|^2)_{\text{av}}\left(\frac{x_s}{1-n_h}\right)^2(1-n_h-x_s)\right].$$

Now $x_d+x_s=x$, and from Fig. 4 we see that for $x\gg n_h$ we have $x_d\simeq n_h$. Thus, using $x_s=x-n_h$ results in

$$\frac{1}{\tau_{s-s}}=\frac{\Omega N_{\text{Pd}}}{2\pi\hbar}k_F^2\left(\frac{dE}{dk}\right)^{-1}_{k=k_F}\times(|\langle v_{\text{D}}(a_s)\rangle|^2)_{\text{av}}\frac{(x-n_h)(1-x)}{1-n_h}, \quad x\gtrsim n_h. \quad \text{(A5)}$$

Substituting the explicit expression for $(|\langle v_{\text{D}}(a_s)\rangle|^2)_{\text{av}}$ leads to Eq. (5).

[15] See Ref. 5, pp. 247ff.